Basic Electrophysiology

1

Victoria M. Robinson and Stanley Nattel

Abstract

Basic electrophysiology is a rapidly evolving field, rich in detail. This introductory chapter provides a succinct and essential overview of key concepts in basic electrophysiology covering: The stages of the cardiac action potential and their generation; Excitation-contraction coupling; Cardiac automaticity; The cardiac conduction system and Arrhythmogenesis, including abnormal automaticity, afterdepolarizations, triggered activity and re-entry.

Keywords

Ion channels • Action potential • Electro-mechanical coupling • Automaticity • Cardiac conduction • Arrhythmogenesis • Afterdepolarisations • Triggered activity • Re-entry • Rotors

Introduction

Basic electrophysiology is a broad and fascinating discipline. To discuss this topic in depth is beyond the scope of a single book chapter. This chapter therefore serves as an introduction to the major areas of basic electrophysiology relevant to the practicing clinician. It is designed to be suitable for a wide range of readers from senior medical students to general physicians and cardiologists. It broadly covers key concepts in action potential formation, automaticity, cardiac conduction and arrhythmogenesis. Note, more detailed discussion into the mechanisms of specific arrhythmias will be addressed in later chapters pertaining to those individual arrhythmias.

V.M. Robinson, M.B.Ch.B. (✉)
Lankenau Institute of Medical Research, Philadelphia, PA, USA

The University of Manchester, Manchester, UK
e-mail: v.m.robinson@icloud.com

S. Nattel, M.D.
Department of Medicine and Research Center, Montreal Heart Institute, Université de Montréal, Montreal, QC, Canada

Department of Pharmacology and Therapeutics, McGill University, Montreal, QC, Canada

Institute of Pharmacology, West German Heart and Vascular Center, University Duisburg-Essen, Duisburg, Germany
e-mail: stanley.nattel@icm-mhi.org

The Cardiac Action Potential

What Is an Action Potential? (AP)

The cardiac action potential (AP) is the time course of voltage change across a cardiac cell membrane, during one cardiac cycle. It is the basis for the electrical impulse that spreads through the heart and initiates organised contraction [1]. The cardiac AP has a specific shape, which varies among different areas in the heart. The ventricular AP, depicted in Fig. 1.1, will be used as the standard exemplar for this chapter.

How Is the Cardiac AP Generated?

Membrane Potential, Equilibrium Potential and Driving Force

To appreciate how the AP is generated, it is important to first understand the concepts of membrane potential (E_m) and equilibrium potential. The membrane potential is the potential difference, or voltage between the cell interior and

P. Kowey et al. (eds.), *Cardiac Arrhythmias, Pacing and Sudden Death*, Cardiovascular Medicine,
DOI 10.1007/978-3-319-58000-5_1

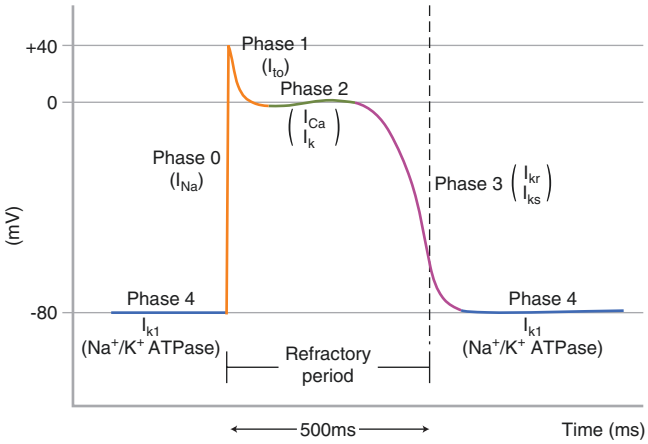

Fig. 1.1 Representative diagram of a ventricular AP, depicting the change in transmembrane voltage over time, as seen from the inside of the cell. The different phases of the AP are labelled along with the principal currents flowing during each phase. See text for details

exterior, and is formed by the unequal separation of charge across the cell membrane.

When a cell is selectively permeable to a specific ion and a concentration gradient is present, that ion species will diffuse down its concentration gradient, leaving behind a charge opposite to that of the permeable ion. The charge will attract the permeable ion back, and when enough charge has built up the electrical force holding the ion back becomes equal and opposite to the chemical force pushing the ion out. The transmembrane voltage at which the electrical and chemical forces exactly oppose each other, so that the ion stops moving, is called the "equilibrium potential". Each ion has a specific equilibrium potential (E_{ion}), calculated by the Nernst equation (Fig. 1.2). The driving force on an ion before the equilibrium potential is reached is equal to the membrane potential minus the equilibrium potential:

Driving Force = ($E_m - E_{ion}$).

In cardiac myocytes, the resting membrane potential is the potential during electrical quiescence between APs, i.e. phase 4 (Fig. 1.1) [2]. During phase 4, the membrane has the highest permeability to K^+ ions, with only slight permeability to other ions, therefore the resting membrane potential of roughly −80 mV lies close to the equilibrium potential for K^+. When the permeability to another ion increases, such as when channels carrying that ion open, e.g. the opening of Na^+ channels during phase 0, the membrane potential moves towards the equilibrium potential for that ion. Cellular depolarization, the cell interior becoming less negative, is due to increased permeability to inward-moving ions like Na^+ and Ca^{2+} with positive equilibrium potentials, whereas repolarization, the cell interior becoming more negative and returning towards the resting potential, is due to increased permeability to outward-moving ions like K^+.

During each AP, Na^+ and Ca^{2+} enter the cell, and K^+ leaves the cell. Since there are about 100,000 APs per day, the small net ion movement in each AP would result in loss of the ionic gradients if not compensated. Therefore, cells have active pumps and transporters, like the Na^+/K^+ ATPase pump, with a respective stoichiometry of 3:2 (3 Na^+ ions pumped out of cells, for every 2 K^+ ions pumped in), which maintain ionic homeostasis.

Channel Gating

Central to the generation of the AP is the opening and closure of specific ion-channels, which regulate the membrane permeability to different ions and shape the AP. For example, phase 0 is generated by the opening of Na^+ channels, which allow the cell to depolarize rapidly towards the Na^+ equilibrium potential. Phase 1 repolarization is caused by the opening and rapid closure of "transient outward" K^+ channels, phase 2 (the plateau) is formed by the opening of Ca^{2+} channels balanced by the maintained opening of several K^+ channels, and phase 3 repolarization is generated by the progressive opening of rapid (I_{Kr}) and slow (I_{Ks}) delayed rectifier K^+-currents (Figs. 1.1 and 1.3). The appropriate opening and closure of the various channels involved is determined by voltage and time dependent "gating".

A detailed discussion of the structure of various ion channels and their exact gating mechanisms is beyond the scope of this overview chapter, but some essential elements will be summarised. Ion channels can be classified according to their gating mechanism: voltage-dependent, ligand-dependent or mechano-sensitive (stretch activated) channels [3]. The majority of cardiac ion channels, including all of the key channels shown in Fig. 1.1, are voltage-gated, meaning that their conductance varies with a change in membrane potential. Changes in membrane potential rearrange the alignment of charged amino acids within the channel, causing conformational changes that allow the channels to open [4]. Opening is time-dependent, varying widely from micro-(10^{-6})-seconds for Na^+ channels to hundreds of milli-(10^{-3})-seconds for delayed-rectifier K^+ channels.

Figure 1.4 shows recordings of Na^+ current, obtained by depolarizing the cell membrane to various voltage steps to mimic different degrees of depolarization. The amount of current gradually increases to a peak and then tails off after about 20 mV, since the step potential at this stage is slowly reaching the equilibrium potential for Na^+ ions, therefore the driving force lessens. All voltage-gated ion channels in the AP activate upon depolarization, with the exception of the "funny" current (I_f), which contributes to pacing in the sinoatrial (SAN) and atrioventricular (AVN) nodes, and activates in response to membrane repolarization (which is one of the reasons it is "funny"). The other "funny" aspect of I_f is its relatively poor selectivity for Na^+ versus K^+,

$$E_{ion} = \frac{RT}{zF} \log_e \frac{[ion]_o}{[ion]_i}$$

Ion	Extracellular Concentration (mM)	Intracellular Concentration (mM)	E_{ion} (mV)	Permeability ratio to K^+ ions at resting potential (P_X/P_K)
K^+	4	120	-90	1.00
Na^+	140	10	+70	0.04
Ca^{2+}	2	0.1-0.5	+131	0.20
Cl^-	100	22	-40	0.11

Fig. 1.2 *Top panel:* The Nernst Equation, where E = equilibrium potential of the ion species in question (mV), R = gas constant (8.314 J K^{-1} mol^{-1}), T = absolute temperature in Kelvin, *z* = valence of ion, F = Faraday constant (96,485 C mol^{-1}), $[ion]_o$ = concentration of the ion on the *outside* of the cell membrane, $[ion]_i$ = concentration of the ion on the *inside* of the cell. *Bottom panel*: Table showing relevant properties of the most important ions in cardiac myocytes [2]

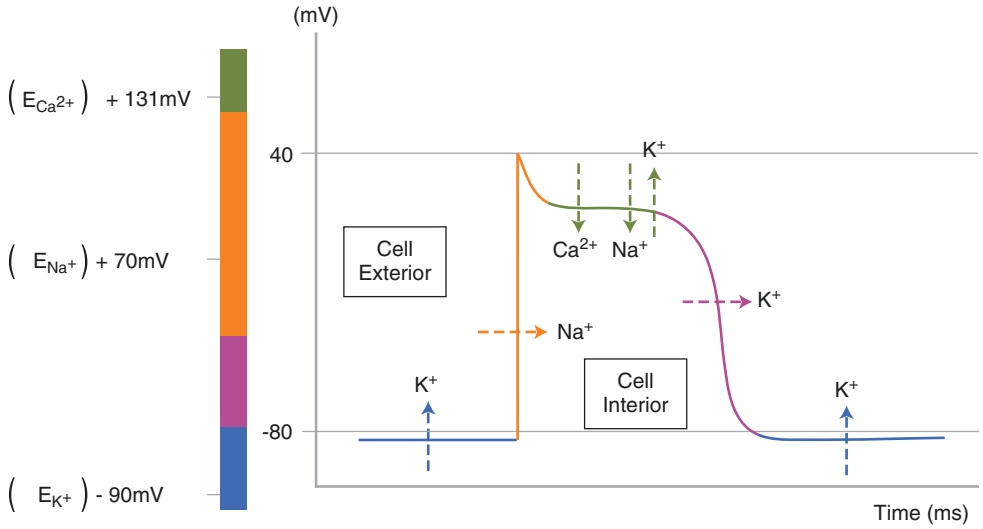

Fig. 1.3 A diagram showing the ventricular AP with the ions able to permeate the membrane during the various AP phases. The colour coding used is identical to that used to show the AP phases in Fig. 1.1 for ease of comparison. The colour bar on the *left* of the panel gives a linear representation of the various equilibrium potentials of the key ion species. Once a membrane is permeable to an ion through channel gating, it is subject to a driving force and diffuses either into or out of the cell down its concentration gradient in an attempt to reach its equilibrium potential. The labels of "cell interior" and "cell exterior" indicate the direction of travel of the different ion species during AP phases

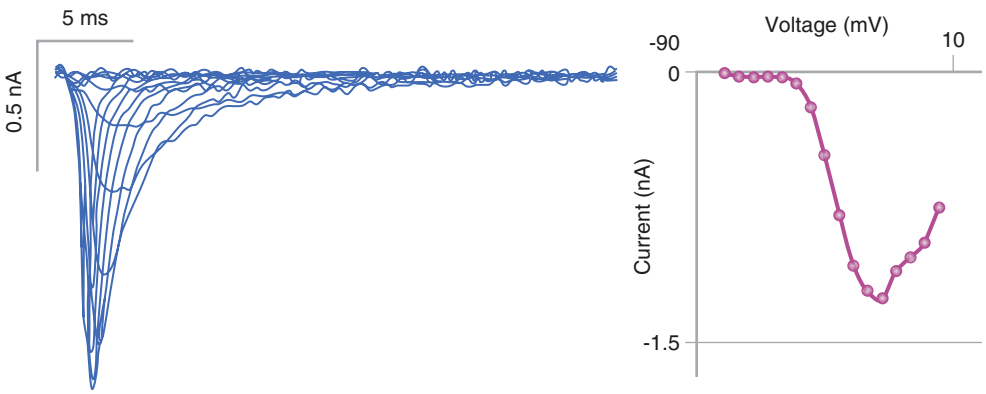

Fig. 1.4 *Left panel* (**a**): Na^+ currents during successive depolarizing voltage steps (test potentials). *Right panel* (**b**): Plot of Na^+ current recorded in nA (y-axis) at each test potential (mV), producing a current-voltage (I-V) curve

resulting in an equilibrium potential between those of Na^+ and K^+, at about −20 mV.

Voltage can also govern the closure of ion channels. Some channels, such as Na^+, transient outward K^+, and Ca^{2+} channels, switch to an inactive state with sustained depolarization (channel inactivation), which stops ion flux through the channel. Currents carried by these channels typically increase and then spontaneously decrease. In order for these channels to be "re-set" so they can be activated again by depolarization, they must first be returned to their resting closed state (recovery from inactivation). Channels that do not manifest inactivation (like the delayed rectifier channels) open in a time-dependent way, and do not close until the cell repolarizes to voltages at which opening is reversed back to the resting potential (deactivation) [3].

Another valuable concept is the phenomenon of rectification. Inward rectifiers conduct inward currents at voltages negative to their equilibrium potential more easily than outward currents at voltages positive to their equilibrium potential. Therefore, with progressive depolarization of the cell membrane, ion flow decreases through inward rectifiers. The most important inward rectifier in the heart is I_{K1}. The inwardly rectifying properties of I_{K1} are particularly important in preventing highly wasteful loss of K^+ from the cell interior during phases 0–2, when positive potentials produce a strong driving force for K^+ egress that would drive large amounts of K^+ out of the cell if I_{K1} permeability remained high.

Stages of the Cardiac AP

Phase 4: the Resting Membrane Potential

When the cardiac myocyte is resting, the outward I_{K1} current is most active, and K^+ ions slowly leak out of the cell in order to drive the membrane down to E_K (−90mv). The high I_{K1} conductance, along with the action of Na^+/K^+ ATPase to prevent the dissipation of the K^+ concentration gradient, keep the resting membrane potential stable at about −80 mV, unless a depolarization event occurs.

Phase 0: The Rapid Upstroke

The arrival of a depolarizing pulse, via propagation initiated by the cardiac pacemaker in the SAN, causes Na^+ channels to open. If the depolarization is large enough, i.e. reaches a threshold potential, Na^+ channels open and Na^+ ions flow down their concentration gradient into the cell, moving the membrane potential to more positive values. Rapid depolarization continues until the equilibrium potential for Na^+ is almost reached. After initial very rapid activation, Na^+-channels inactivate rapidly, contributing to termination of the AP upstroke. Na^+-channels then remain inactive until the membrane is repolarized, towards the end of phase 3, producing the absolute refractory period (Fig. 1.1).

The depolarization of the cell during phase 0 provides the large amount of energy needed for rapid conduction. The reduction of Na^+-current by antiarrhythmic drugs or Na^+-channel mutations leads to conduction slowing [5]. The electrocardiographic QRS duration reflects the time for the ventricles to be electrically activated, therefore ventricular conduction slowing is reflected by QRS prolongation.

Phase 1: Early Repolarization

The repolarizing notch that forms phase 1 of the AP is largely mediated by the transient outward current (I_{to}), primarily carried by a rapidly activating and inactivating K^+-channel. Phase 1 sets the membrane potential level for phase 2, thereby governing the degree of Ca^{2+} entry during the AP plateau [3]. Excessive dominance of I_{to} over opposing inward currents (especially residual I_{Na}) is important in the pathogenesis of J wave syndromes like the Brugada Syndrome [6], as detailed in Chap. 4.

Phase 2: The AP Plateau

A balance between inward current (mainly L-type Ca^{2+} current, I_{CaL}) and outward current (mainly I_{K1}, but also the delayed rectifiers I_{Kr} and I_{Ks} in the later stages of phase 2) maintains the AP plateau. The major role of the phase-2 inward Ca^{2+}-current is to produce Ca^{2+}-induced- Ca^{2+} release from the sarcoplasmic reticulum, i.e. the Ca^{2+} transient that leads to muscle contraction (see section "Contraction of Cardiac Myocytes"). Other inward currents include the late Na^+ current (INa_{-L}), which is believed to be a composite of delayed inactivation and re-opening of some Na^+ channels [2]. The Na^+-Ca^{2+} exchanger (NCX) contributes secondarily to the inward plateau current [7] since it is electrogenic: 3 Na^+ ions are transported into the cell, for every 1 Ca^{2+} ion exported out, leaving one net positive charge inside the cell. This is termed the "forward" mode of the NCX and is the usual direction of ion transport. Towards the end of phase 2, the inward currents begin to inactivate and the outward delayed rectifier currents, which are activated more slowly by depolarization become more prominent.

The QT interval on an ECG indicates the time from ventricular activation (QRS) to repolarization (T wave), and is an index of AP duration (APD). Imbalances between inward and outward currents during phase 2, can lead to pathological lengthening or shortening of the QT interval [8–11]. The pathophysiology of such syndromes is discussed in Chap. 4.

Phase 3: Repolarization

I_{Kr} is the major current directing repolarization during phase 3. I_{Ks} activates too slowly to play a major role during normal APs and its main role is as a "safety valve", increasing appreciably to prevent excessive AP-prolongation when repolarization is challenged (e.g. by APD-prolonging drugs or when I_{CaL} is enhanced by adrenergic stimulation). As the membrane potential repolarizes to below −20 mV, I_{K1} increases and contributes to late phase 3 as inward rectification is removed.

Contraction of Cardiac Myocytes

Ca^{2+}-Induced Ca^{2+} Release

The L-type Ca^{2+} channels are primarily located in the transverse tubules (T tubules), which are deep invaginations of the cardiomyocyte membrane (Fig. 1.5) [12]. T tubules are in close physical proximity to the sarcoplasmic reticulum (SR), the organelle that stores and releases intracellular Ca^{2+}. The SR has outpouchings, called junctional SR cisternae, which resemble flattened sacks reaching out towards the T-tubule extensions, in which are located clusters of ryanodine receptor Ca^{2+} release channels (RyRs) [13]. Ca^{2+} ions entering the cell can therefore quickly activate RyRs, causing a large release of Ca^{2+} from the SR into the cytoplasm, a process called "Ca^{2+}-induced- Ca^{2+} release" (CICR). The area of cytoplasm in which the T tubules and the SR come into close proximity is called the dyadic cleft.

Excitation-Contraction Coupling

The Ca^{2+} released into the cytosol by CICR binds to the myofilament protein regulator troponin-C [13]. Ca^{2+} binding to troponin-C causes a conformational change [14], followed by complex interactions with troponin-I, troponin-T and tropomyosin, exposing the myosin binding sites on actin and allowing cross-bridge cycling to take place [15].

The intracellular Ca^{2+} released during systole is removed from the cytoplasm during diastole, causing cardiac relaxation. The principal removal mechanisms are the Sarcoendoplasmic Reticulum Calcium ATPase (SERCA), which pumps Ca^{2+} back into the SR, and the NCX, which exports Ca^{2+} across the cell-membrane, Fig. 1.5).

Automaticity: The Cardiac Pacemakers

Cells with pacemaker activity spontaneously generate electrical signals. To do this, they depolarize automatically during phase 4 to the threshold potential required to initiate an AP (Fig. 1.6).

The intrinsic firing rate of roughly 60–75/min in the sinoatrial node (SAN) is faster than the other pacemaker regions (His-Purkinje system: 30–40/min, atrioventricular node (AVN) 40–50/min). The SAN is therefore the predominant pacemaker in the heart. The other regions possessing spontaneous automaticity act as back-up pacemakers, taking over if pacing fails in the SAN. There

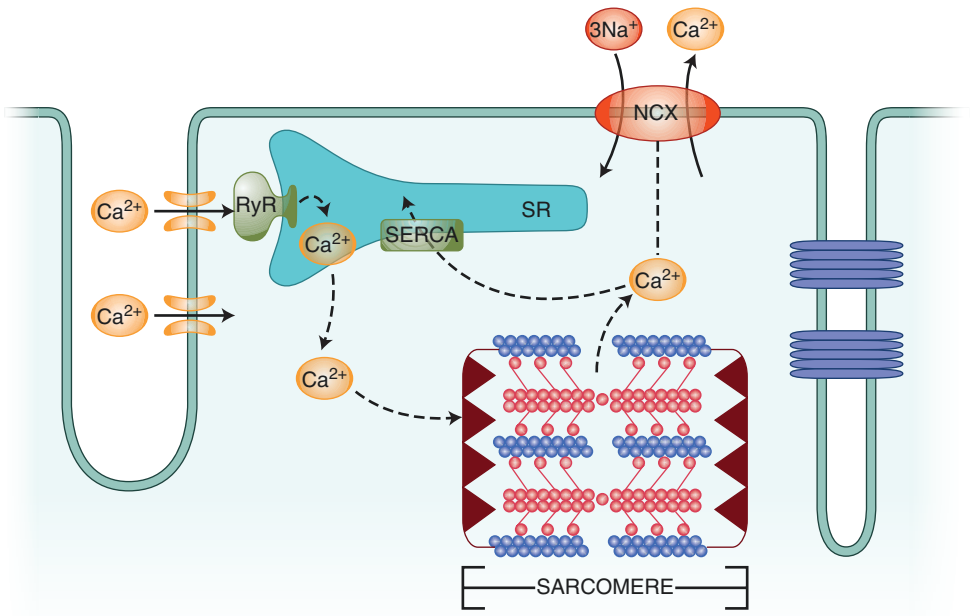

Fig. 1.5 Diagram of Ca^{2+}-induced Ca^{2+} release. L-type Ca^{2+} channels allow Ca^{2+} to activate ryanodine receptors in the dyadic cleft, triggering a larger release of Ca^{2+} into the cytoplasm. This Ca^{2+} causes contraction of the sarcomere. Ca^{2+} removal from the cytoplasm during diastole (via uptake into the SR by the SERCA pump and export from the cell via NCX) causes cardiac relaxation

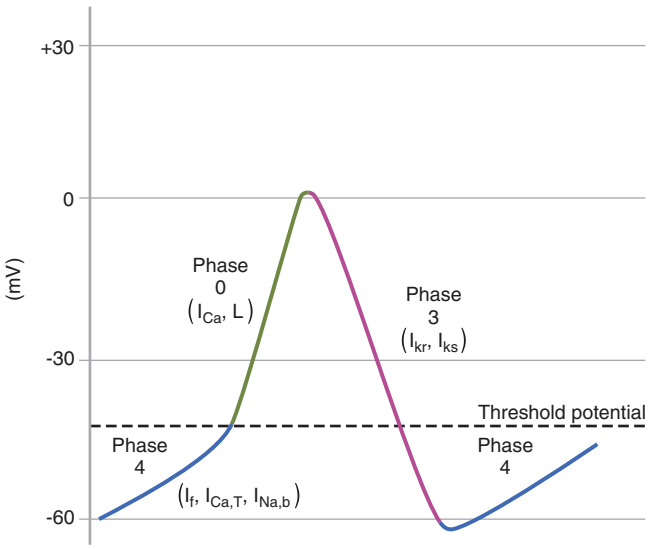

Fig. 1.6 Representative diagram of a spontaneous AP in the SAN

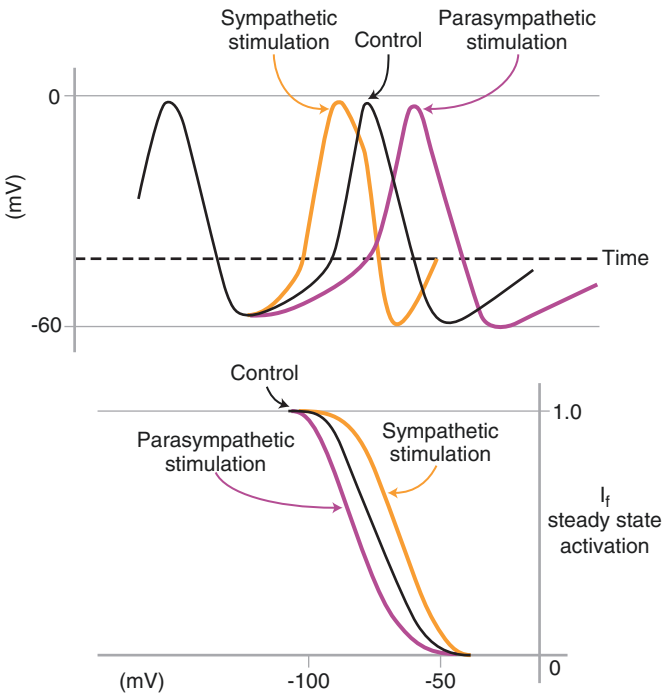

Fig. 1.7 *Top panel*: diagram showing the effect of the autonomic nervous system on the rate of phase 4 diastolic depolarization and therefore heart rate. *Bottom panel*: diagram showing the effect of the autonomic nervous system on the activation curves and therefore channel availability of HCN4 channels (I_f current). Adapted from [18]

are two principal mechanisms contributing to phase-4 diastolic depolarization, the membrane clock and the Ca^{2+} clock.

The Membrane Clock Model

The membrane clock involves a set of inward currents working together to depolarize the membrane to threshold. The best-known ion-channels involved in pacemaker activity are the hyperpolarization-activated cyclic nucleotide-gated channels (HCN channels), which underlie I_f [16]. Although these channels structurally resemble the K^+ channel superfamily, they are also permeable to Na^+ and to a lesser extent, Ca^{2+} [17]. At physiological voltages, Na^+ influx is greater than the outward K^+ current through HCN4 channels, which acts to gradually depolarize the cardiomyocyte to threshold as the I_f current.

The autonomic nervous system strongly regulates I_f. Sympathetic activation increases intracellular levels of cyclic AMP (cAMP), which binds to the cyclic-nucleotide binding domain at the C-terminus of the channel. Binding of cAMP to HCN4 causes a "rightward-shift" in the I_f activation curve, increasing the current flowing through the channel, and consequently the rate of phase-4 depolarization, at any given voltage (Fig. 1.7, *bottom*) which causes an increase in heart rate in response to sympathetic agonists (Fig. 1.7, *top*). The parasympathetic nervous system reduces the concentration of intracellular cAMP, causing a "leftward-shift" in the voltage-dependence of activation for I_f and a reduced phase-4 slope (Fig. 1.7).

Pathological loss of function of HCN4 can lead to the sick sinus syndrome [17]. Another poorly selective inward current has been described in rabbit, rat and guinea pig SAN cells, and flows despite I_f blockade with cesium [19]. This cation channel has its greatest permeability to Na^+ ions and has therefore been labeled as carrying the "background Na current" ($I_{Na,b}$) [17]. $I_{Na,b}$ is activated at −60 to −70 mV and has a peak current at about −50 mV, therefore is thought to work in synergy with the I*f* to achieve diastolic depolarization as part of the membrane clock [17]. Ca^{2+} channels also contribute to the membrane clock. L-type Ca^{2+} (Ca_v 1.2) channels activate at about −30 mV and therefore do not contribute to phase 4 of the SAN AP. However, another subfamily of voltage gated Ca^{2+} channels, T-type Ca^{2+} channels (Ca_v 3.1 and 3.2) are activated at roughly −60 mV [17] and therefore contribute to diastolic depolarization. The L-type Ca^{2+} channels present in SAN cells are primarily responsible for the phase 0 upstroke of the AP, therefore they determine SAN-cell threshold and automatic rate.

Additional ion channels are involved in regulating the membrane clock and diastolic depolarization under particular circumstances. I_{KACh} and I_{KATP} are inward-rectifier K^+ currents expressed in the SAN [17]. I_{KACh} channels open in response to acetylcholine release from vagal nerves, which activates muscarinic receptors in the SAN [20, 21]. The hyperpolarizing effect of acetylcholine reduces SAN pacing rate by moving diastolic potentials further from threshold [22]. I_{KATP} similarly hyperpolarizes the myocyte

membrane and is activated in response to reduced intracellular ATP levels, as occurs in myocardial ischaemia and hypoxia [23].

The Ca^{2+} Clock Model

Spontaneous SR Ca^{2+} release produces Ca^{2+} sparks or waves [24], which can propagate throughout the cell. Such Ca^{2+} sparks and waves near the edge of rabbit SAN myocytes produce Ca^{2+} transients that precede the SAN AP (Fig. 1.8). The released Ca^{2+} is extruded through the NCX, which carries a depolarizing inward current when removing Ca^{2+} from the cell. This inward current depolarizes the cell and contributes to SAN phase 4 depolarization. Suppressing Ca^{2+} sparks and waves decreases the slope of diastolic depolarization, particularly later in phase 4, and inhibits spontaneous SAN firing [25]. The automatic mechanism resulting from inward NCX-current resulting from spontaneous SAN Ca^{2+} release is called the "Ca^{2+} clock".

While Ca^{2+} sparks and resultant inward current oscillations via NCX can occur in the absence of APs, they dissipate over time without APs, which act to cyclically regulate cellular Ca^{2+} stores needed to maintain the Ca^{2+} clock. Thus, the membrane clock and the Ca^{2+} clock act co-dependently to achieve spontaneous diastolic depolarization and maintain automaticity.

Other Currents

Other currents may also contribute to SAN function. For example, there is evidence that the intermediate-conductance Ca^{2+}-activated K^+ channel ($K_{Ca}3.1$) may be important for SAN membrane depolarization upon initial Ca^{2+} entry/release [17]. This effect might contribute to maintaining membrane-voltage cycling between negative values (in the absence of significant SAN I_{K1}) and more positive values due to membrane and/or Ca^{2+} clock-induced depolarization.

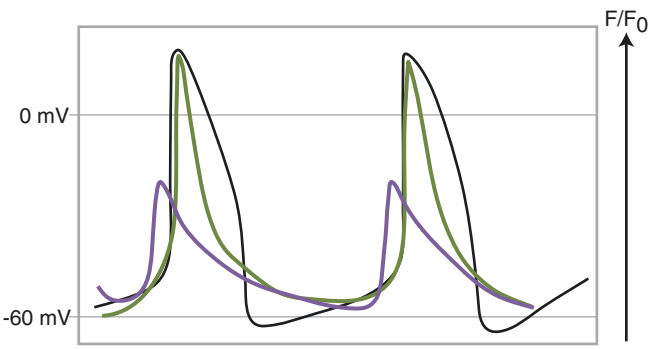

Fig. 1.8 Superimposed AP plots (*black line*) upon Ca^{2+} fluorescence transients measured by confocal microscopy in rabbit sinoatrial nodal cells. The *purple line* indicates the Ca^{2+} transient measured towards the edge of the cells, which precedes the major Ca^{2+} transient produced during phase 2 of the AP (green line). Adapted from [25]

Cardiac Conduction

SAN pacemaker activity initiates the cardiac impulse. The wave of depolarization travels through the atria, likely via organized strands of cardiomyocytes called the internodal pathways, since the three bundles track anteriorly, medially and posteriorly to the atrioventricular node (AVN). The anterior internodal pathway branches to form Bachmann's bundle, which crosses to the left atrium [26]. From these preferential conduction pathways, myocardial depolarization spreads more slowly through the remainder of the atrium. Atrial activation corresponds to the electrocardiographic P-wave.

Once the depolarizing impulse reaches the AVN, the wave of depolarization traverses slowly to reach the cable-like His-Purkinje system (Fig. 1.9) before spreading to the ventricles. This delay allows adequate time for ventricular filling after atrial contraction, before ventricular systole begins. The P-R interval represents the time for conduction to spread between the SAN and the ventricles.

After the depolarizing impulse has passed through the AVN, it travels via the bundle of His in the interventricular septum to the bundle branches and the Purkinje network, and from there spreads to activate the ventricles and produce the QRS complex. Finally, ventricular repolarization occurs, corresponding to the T-wave on the ECG.

Unlike APs in the working atria and ventricles/His-Purkinje system, the APs of the SAN and AVN have depolarized resting potentials; slow phase-0 upstrokes mediated by Ca^{2+} currents and delayed recovery of excitability governed by slow Ca^{2+} current recovery kinetics. Accordingly, the 2 types of APs are referred to as "fast-channel" (in working atria-ventricles/His-Purkinje system) and "slow-channel" (in SAN and AVN). The slower recovery kinetics of the Ca^{2+} channel and the resultant prolonged refractory period in the AVN allows the AVN to protect the ventricles against rapid conduction of supraventricular tachyarrhythmias. The main differences between fast and slow-channel APs are summarized in Table 1.1.

The AVN has a complex 3-dimensional structure. The core of the AVN is composed of pure slow-channel tissue ("N"-cells), while towards the atrial and ventricular ends, transitions are seen towards more "atrial-like" (AN) and "ventricular-like" (NH) APs. Mutations in SCN5A, the principal gene encoding Na^+ channels, can slow AVN conduction in humans by virtue of transitional AVN cells that possess significant Na^+ current [27].

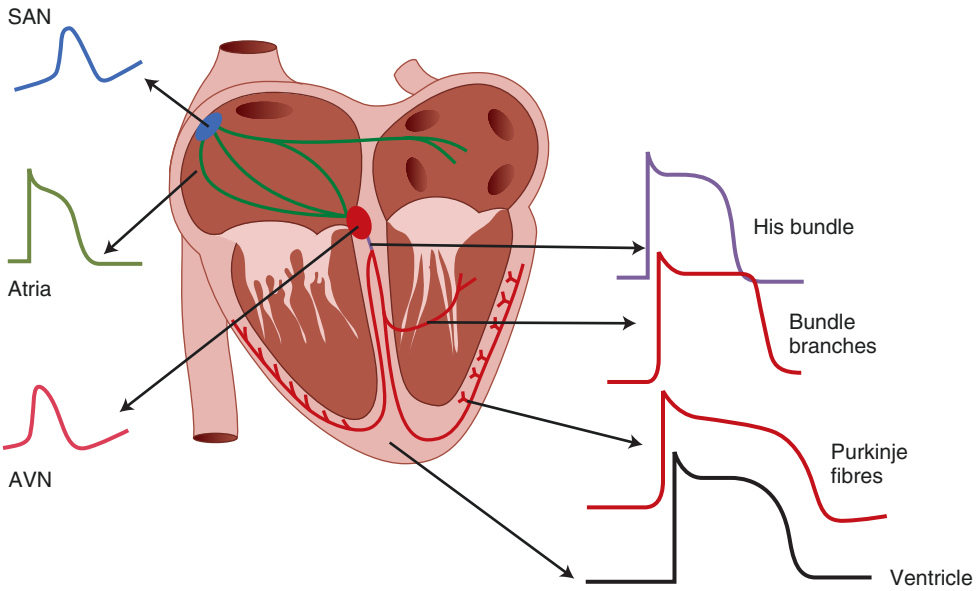

Fig. 1.9 Diagram of the principal components of the cardiac conduction system and their corresponding APs. Sinoatrial node (*blue*), internodal pathways and Bachmann's bundle (*green*), atrioventricular node (*red*), bundle of His (*purple*), bundle branches and purkinje fibres (*red*)

Table 1.1 Summary of the key differences between fast and slow-type APs.

	Fast-channel AP	Slow-channel AP
Phase 0 Conduction mediated by	Na^+ channels	Ca^{2+} channels
Activation	Fast	Fast
Recovery	Slow	Slow
Refractoriness determined by	AP Duration	Ca^{2+} channel recovery time

The N cells are the principal pacemaker cells within the AVN, and exhibit typical slow-channel AP morphology. N cells have a relatively positive diastolic membrane potential due to a very low density of I_{K1} [28], favoring pacemaker activity that allows the AVN to act as an "escape" pacemaker if the SAN fails. N cells also possess significant expression of a second isoform of L-type Ca^{2+} channels, Ca_v 1.3 channels, as opposed to the Ca_v 1.2 isoform found in atrial and ventricular myocytes [29, 30]. Ca_v 1.3 channels have a more negative activation potential than Cav 1.2 channels, and can activate towards the end of phase 4 to facilitate AVN automaticity. Ca_v 3.1, encoding the alpha-subunit of T-type Ca^{2+} channels, is also highly expressed in the AVN and contributes to automaticity [30].

Cell-Cell Coupling

The atrial and ventricular myocytes are connected to each other so that the wave of depolarization can rapidly spread throughout the myocardium as a functional syncytium and allow the heart to contract in a coordinated manner. The specialised area connecting myocytes electrically is called the intercalated disc. Three principal structures make up the intercalated disc: (1) adherins junctions, which provide anchoring sites for actin/sarcomeres, (2) desmosomes, structural proteins that bind cells together and (3) gap junctions; conduits between cells that contain cylindrical connexons joining cells, each connexon being composed of six interlinked connexin molecules [31]. Each connexin molecule is a hemichannel that connects to another connexin molecule in an adjacent cell, to form a low-resistance water-filled pore between the cells through which a propagating cardiac impulse can easily travel.

There are different isoforms of connexins within the myocardium. The ventricles primarily contain Cx43; the atria, a combination of Cx40 and Cx43; the AVN contains Cx45 and possibly Cx31.9; the Purkinje system Cx40, Cx43 and Cx45. Connexons can form with the same isoform (homotypic) or a mixture of isoforms (heterotypic). *D*isruption of gap junction number or distribution, or gap junction dysfunction, impairs cardiac conduction and predisposes to arrhythmia.

Connexins interact with other molecules within the intercalated disc, especially with desmosomal proteins, regulatory proteins and ion channels, forming macromolecular complexes that coordinate electrical propagation within the syncytium [32]. For example, Cx43 and the principal Na^+ channel isoform $Na_v1.5$ colocalise in the intercalated disc [33]. Desmosomal proteins also have important regulatory roles. For example, a reduction in the desmosomal protein plakophilin-2 significantly reduces Na^+ current at the intercalated disc [34]. It is therefore not only connexins that allow electrical propagation within the syncytium, but the coordinated interaction of several proteins within the intercalated disc.

Arrhythmogenesis

Arrhythmogenesis can be broadly divided into two categories: (1) reentry, in which a propagating impulse persists by continuous re-excitation in a re-entrant pathway, and (2) abnormal impulse formation, which can be subdivided into abnormal automaticity and triggered activity (Fig. 1.10).

Abnormal Automaticity

Abnormal automaticity encompasses enhanced automaticity in pacemaker tissue, or the generation of spontaneous activity in atrial or ventricular myocytes that do not normally spontaneously depolarize. Examples of arrhythmias caused by abnormal automaticity are focal atrial tachycardia, nonparoxysmal junctional tachycardia and accelerated idioventricular rhythm [35]. Abnormal automaticity is generally observed in situations creating a more positive resting membrane potential, which allows phase 4 diastolic depolarization to reach threshold faster.

Afterdepolarizations and Triggered Activity

Afterdepolarizations can be early (EADs) or delayed (DADs). They are transient depolarizations occurring during phases 2 or 3 of the AP (EADs) or following full repolarization in phase 4 (DADs). When the amplitude of afterdepolarizations is sufficient to bring the membrane potential to threshold, spontaneous APs known as triggered beats or triggered activity can occur.

Early Afterdepolarizations (EADs)

EADs occur when the AP is prolonged by a decrease in outward currents or an increase in inward currents. This can result in the reactivation of the L-type Ca^{2+} channel current ($I_{Ca,L}$), since L-type Ca^{2+} channels have a significant overlap between the activation and inactivation vs. voltage curves between potentials of about −30 mV and 0 mV, providing a voltage-range in which there is steady-state depolarizing inward Ca^{2+}-current (the so-called "window current", Fig. 1.11) [36]. The window-current voltage range corresponds to the AP plateau, therefore if the AP plateau is sufficiently prolonged, L-type Ca^{2+} channels can recover from inactivation and subsequently re-activate [37], causing an EAD.

Prolonged repolarization can be achieved by: [1]

1. Inhibiting I_{Ks} and I_{Kr} (e.g. Long QT syndrome Type 1 and 2 respectively, ion-current remodelling in heart failure, and with class Ia and III antiarrhythmic drugs).
2. Increasing the availability/amplitude of $I_{Ca,L}$ (e.g. sympathetic nervous system activation).
3. Increased NCX (e.g. with increased intracellular Ca^{2+} or NCX upregulation as in heart failure).
4. Increased late Na^{+} current (e.g. Long QT syndrome Type 3).

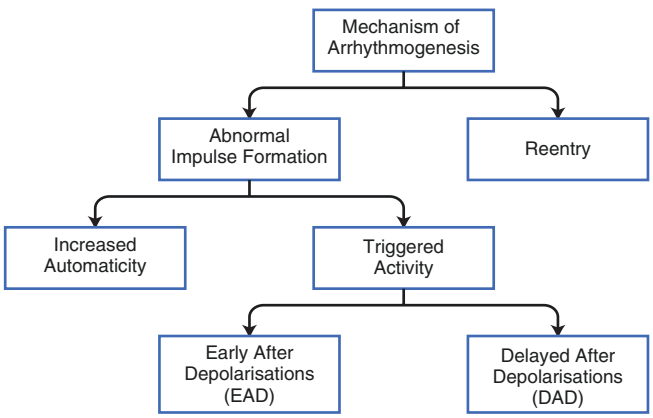

Fig. 1.10 Classification of arrhythmogenic mechanisms

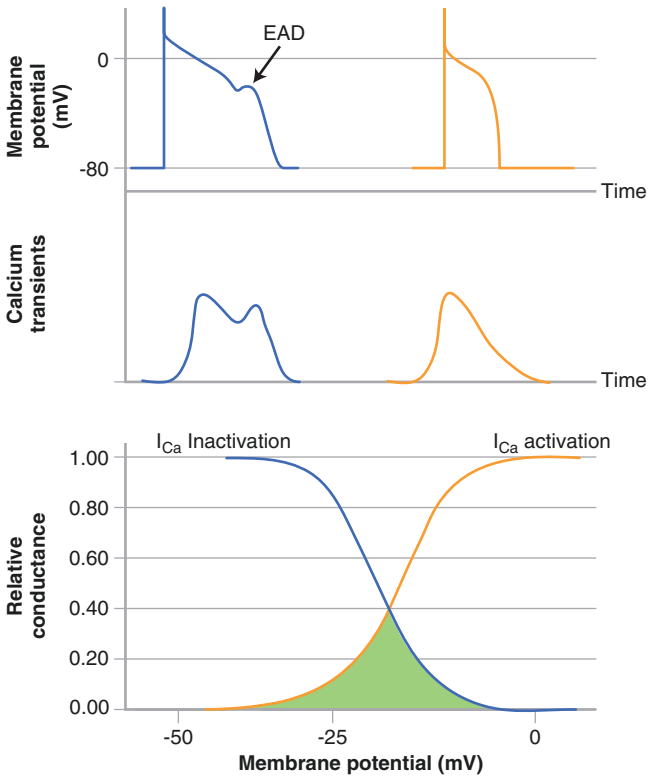

Fig. 1.11 *Top panel*: Diagram of an early afterdepolarization formed during a prolonged AP and the corresponding reactivation of Ca^{2+} depicted below it. To the right is a normal AP, with a single Ca^{2+} transient i.e. no reactivation of the Ca^{2+} current is present. *Bottom panel*: Superimposed activation and inactivation curves for the Ca^{2+} current. The overlapping area shows the window current. Adapted from [2]

EADs preferentially occur in the His-Purkinje system, depolarizing adjacent atrial or ventricular muscle to the threshold for Na^+ channel activation, which in turn can cause triggered beats and tachyarrhythmias.

Delayed Afterdepolarizations (DADs)

DADs are caused by abnormal diastolic release of Ca^{2+} from the SR via RyRs [38, 39]. The released Ca^{2+} is extruded from the cell by NCX, with each Ca^{2+} ion exchanged for 3 extracellular Na^+ ions, producing a net inward current that depolarizes the membrane and causes the DAD [38, 39]. DADs that reach threshold cause premature beats, which can occur singly, can trigger reentry in a vulnerable substrate, and can occur in repetition causing a focal tachyarrhythmia. Arrhythmias induced by DADs include catacholaminergic polymorphic ventricular tachycardia (CPVT), paroxysmal atrial tachycardia, fascicular tachycardia and the bidirectional VT that can be seen in digoxin toxicity [35].

Reentry

Anatomical Reentry

The simplest form of reentry is *circus movement reentry*, in which a cardiac impulse travels in a circuit around a fixed anatomical barrier (Fig. 1.12). In the left panel of the figure, the excitatory wave front travels anterogradely (the usual direction of conduction) down both pathways B and C, and clashing wave fronts cancel each other out. In the right panel, a premature impulse arrives at pathway C when it is refractory from the prior sinus beat, whereas pathway B (which has a shorter refractory period) has recovered excitability and can conduct the impulse. After reaching the distal end of pathway B, the impulse can travel retrogradely up pathway C. If this wavefront is timed in such a manner that when it reaches the beginning of the circuit again and pathway B is no longer refractory, the same wavefront can travel anterogradely down pathway B again, and continue travelling repetitively in a circuitous manner, as long as the tissue ahead of the advancing wavefront has recovered its refractoriness at all points in the circuit.

Examples of this type of reentry around an anatomical obstacle include the supraventricular tachycardias: atrioventricular reentry tachycardia (AVRT), involving a congenital accessory pathway and atrioventricular nodal reentry tachycardia (AVNRT), in which separate pathways exist within the AVN node and form a potential reentry circuit analogous to the circus movement (ring) model of reentry. Experimental atrial flutter is also an example of anatomical reentry, in which the tricuspid annulus forms the anatomical obstacle. Clinical atrial flutter does not appear to involve an anatomical obstacle.

Certain conditions are needed for this form of reentry to occur. For the propagation to continue, there must always be a portion of the circuit ahead of the moving wavefront that

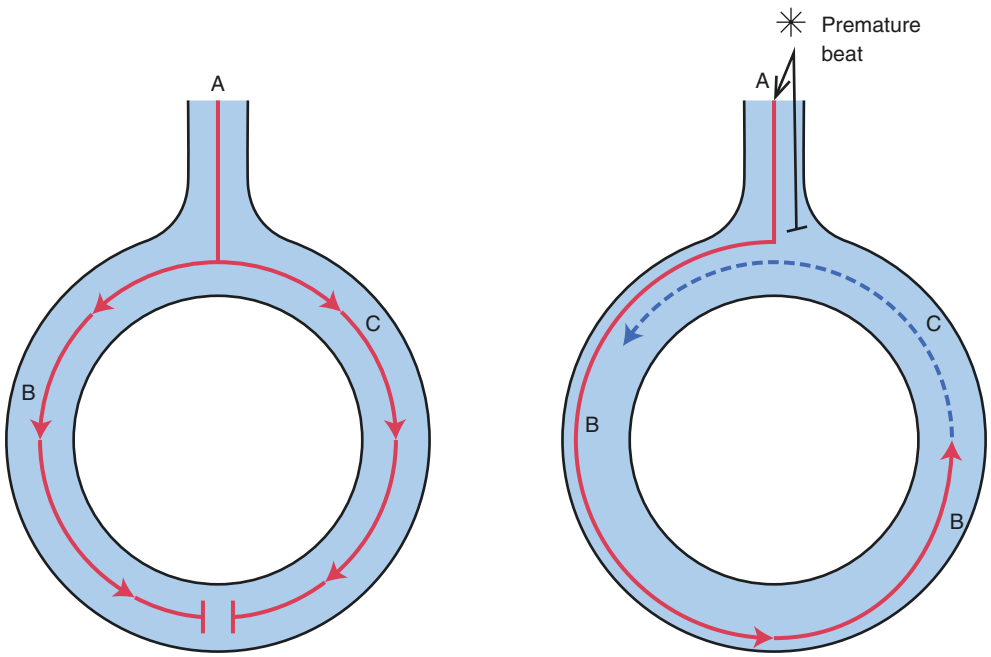

Fig. 1.12 *Left*: diagram showing a cardiac impulse anterogradely propagating down two converging pathways and colliding. *Right*: Reentrant activity as a result of a premature impulse encountering a recovered pathway (*B*) and a pathway (*C*) that is still refractory from the previous sinus beat. The premature impulse conducts anterogradely down pathway *B* and retrogradely up pathway *C* when it has recovered excitability and can continue to propagate around both pathways provided the tissue ahead of the advancing wavefront has recovered its refractoriness

has recovered its excitability, allowing the wavefront to advance. This segment of the circuit is called the *excitable gap* (Fig. 1.13 *left*). The entire length of the circuit (path-length) must equal or exceed the *wavelength*, which is the refractory section of the circuit occupied by the wavefront. Because the wavelength is the distance travelled by a cardiac impulse in one refractory period, it is the shortest distance that can maintain reentry. In mathematical terms, the wavelength is calculated as:

Wavelength = Conduction Velocity × Refractory Period.

Functional Reentry

Reentry can occur in the absence of an anatomical obstacle, on a strictly functional basis. In the 1970s, Allessie *et al.* [41] developed a theory called "the leading circle" (Fig. 1.13, *right*) to account for functional reentry. The authors showed that premature stimuli preferentially travelled in the direction of shorter refractory periods, which led to an arc of refractory tissue, around which a propagating wave front could circulate in the form of reentry. The tissue in the centre of the circle is kept functionally refractory by continuously invading centripetal waves and keeps them from propagating through and interrupting the circulating wavefront. The size of the reentry circuit is determined by the wavelength, because functional reentry naturally establishes itself in the fastest/smallest circuit possible, which has a dimension equal to the wavelength [41]. An advantage of this model is the ability to relate its determinants to familiar and clinically quantifiable concepts also used to describe circus movement reentry such as conduction velocity, refractory period, wavelength and excitable gap. According to the leading circle theory, the persistence of AF depends on the wavelength being reduced so that it is short enough to allow multiple simultaneous reentry circuits to coexist and make AF very stable [42]. Antiarrhythmic drugs stop AF by increasing the wavelength [42].

A problem with the leading circle model is that it fails to account for some important clinical phenomena. For example, in many AF patients and experimental AF models, the wavelength is not reduced and yet AF occurs [43]. In addition, according to the leading circle model, Na^+ channel blocking antiarrhythmic drugs should promote AF by slowing conduction and reducing the wavelength; yet clinically

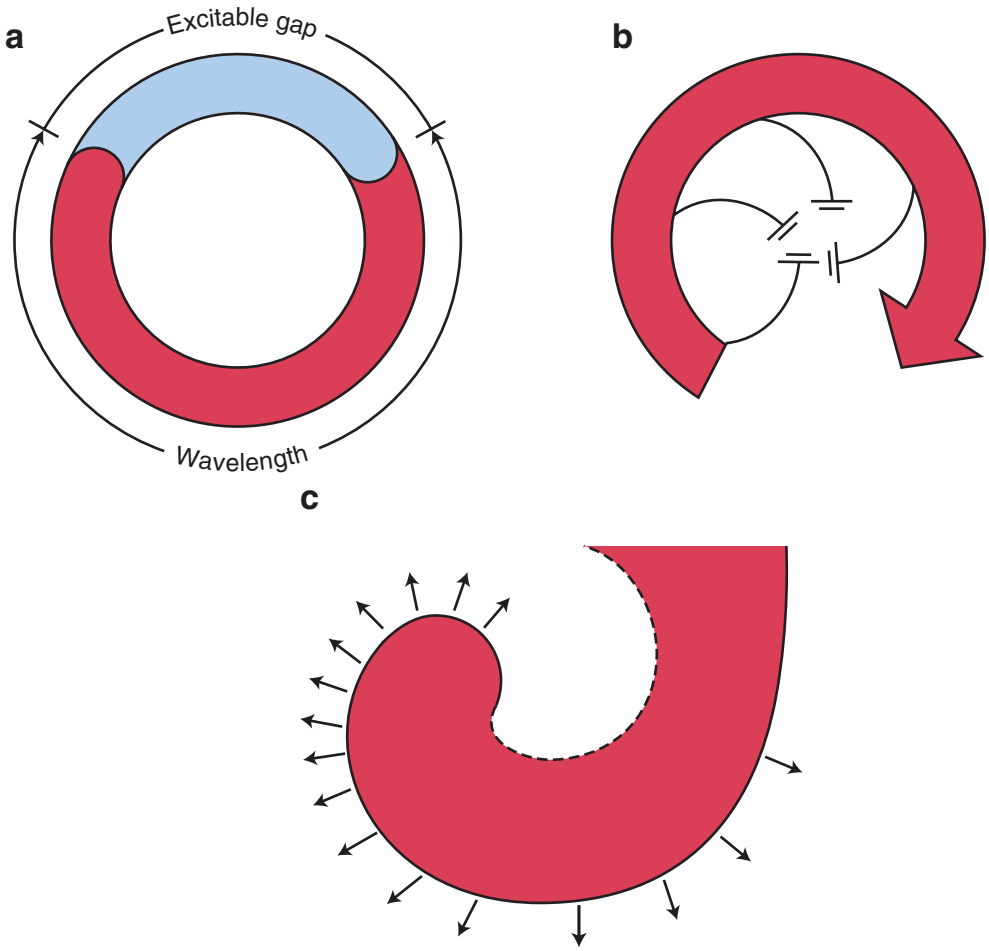

Fig. 1.13 *Left*: Circus movement re-entry (ring model), showing the presence of an excitable gap which is necessary for wave propagation. *Right*: The leading circle model of re-entry. An arc of refractory tissue occurs due to interacting wavefronts. *Bottom*: Spiral wave or rota. The *solid line* represents the depolarizing wave front and the *dashed line* the repolarizing front. Adapted from [40]

they clearly suppress AF [44]. An alternative model of functional reentry is based on the notion of the spiral wave (Fig. 1.13, *bottom*) [40].

The spiral-wave (or "rotor") concept governs reentry-type activity in many systems; a naturally occurring example being a tropical storm (hurricane, typhoon, cyclone) or a spinning top. The persistence of rotational activity depends on the stability of the reentry source, which is governed by the ability of the re-entrant wavefront to constantly propagate through the medium. The ability to propagate depends on the energy of the propagating force, roughly reflected by the speed and tightness of its angular rotation, and the resistance of the medium in front of it to activation, reflected by the amount of energy needed for activation. In cardiac tissue, the rotational "force" is related to the balance between the driving current (generally Na^+ current, the current source), and the resistance to activation, also called the current sink. The current sink is primarily determined by tissue excitability, of which refractoriness is a major determinant.

The analogy of a spinning top can be used to conceptualise rotors. If a spinning top spins quickly, it remains stable. As it begins to slow, its oscillations become larger and it begins to meander and eventually topples over and stops. This helps to understand how reducing the energy and speed of propagation (e.g. by Na^+ channel blockers) can stop reentry maintained by rotors. On the other hand, if the position of a top is stabilized (e.g. by putting a hole in the table which anchors it) it can maintain itself at slower speeds. This may be analogous to the anchoring effect of structural complexities, like tissue fibrosis, that may help to anchor and stabilize AF-maintaining rotors.

The spiral-wave rotor concept is much more successful in accounting for the effects of antiarrhythmic drugs in AF than the leading circle model [40, 44, 45]. In addition, when functional reentry is observed with very high-resolution optical mapping, it takes the form of a spiral wave. Finally, recent technological developments have allowed for the high-resolution mapping of AF in conscious patients, and have provided strong evidence for the existence and presence of rotor activity during AF maintenance in patients [46–49].

Conclusion

This chapter has covered the basics of action potential formation, excitation-contraction coupling of cardiac myocytes, automaticity, cardiac conduction and arrhythmogenesis. The intention is for readers to use this information as a basic reference, upon which to build the more detailed knowledge contained in subsequent chapters.

Acknowledgments The authors would like to thank Dr. Charles Pearman from The University of Manchester for kindly providing the material used to make Fig. 1.4.

References

1. Grant A, Carboni M, Antzelevitch C, Burashnikov A. Cardiac arrhythmia: mechanisms, diagnosis, and management. 2nd ed. Philadelphia: Lippincott Williams and Wilkins; 2001.
2. MacLeod K. An essential introduction to cardiac electrophysiology. 1st ed. London: Imperial College Press; 2014.
3. Grant AO. Cardiac ion channels. Circ Arrhythm Electrophysiol. 2009;2(2):185–94.
4. Zipes D, Jalife J. Cardiac electrophysiology: from cell to bedside. 6th ed. Philadelphia: Elsevier; 2014.
5. Papadatos GA, Wallerstein PM, Head CE, et al. Slowed conduction and ventricular tachycardia after targeted disruption of the cardiac sodium channel gene Scn5a. Proc Natl Acad Sci U S A. 2002;99(9):6210–5.
6. Antzelevitch C, Yan GX. J-wave syndromes: Brugada and early repolarization syndromes. Heart Rhythm. 2015;12(8):1852–66.
7. Whalley DW, Wendt DJ, Grant AO. Basic concepts in cellular cardiac electrophysiology: part I: ion channels, membrane currents, and the action potential. Pacing Clin Electrophysiol. 1995;18(8):1556–74.
8. Huang FD, Chen J, Lin M, Keating MT, Sanguinetti MC. Long-QT syndrome-associated missense mutations in the pore helix of the HERG potassium channel. Circulation. 2001;104(9):1071–5.
9. Lupoglazoff JM, Denjoy I, Berthet M, et al. Notched T waves on holter recordings enhance detection of patients with LQt2 (HERG) mutations. Circulation. 2001;103(8):1095–101.
10. Brugada R, Hong K, Dumaine R, et al. Sudden death associated with short-QT syndrome linked to mutations in HERG. Circulation. 2004;109(1):30–5.
11. Gaita F, Giustetto C, Bianchi F, et al. Short QT syndrome: a familial cause of sudden death. Circulation. 2003;108(8):965–70.
12. Pfeiffer ER, Tangney JR, Omens JH, McCulloch AD. Biomechanics of cardiac electromechanical coupling and mechanoelectric feedback. J Biomech Eng. 2014;136(2):021007.
13. Bers DM. Cardiac excitation-contraction coupling. Nature. 2002;415(6868):198–205.
14. Kobayashi T, Solaro RJ. Calcium, thin filaments, and the integrative biology of cardiac contractility. Annu Rev Physiol. 2005;67:39–67.
15. Gordon AM, Homsher E, Regnier M. Regulation of contraction in striated muscle. Physiol Rev. 2000;80(2):853–924.
16. Garcia-Frigola C, Shi Y, Evans SM. Expression of the hyperpolarization-activated cyclic nucleotide-gated cation channel HCN4 during mouse heart development. Gene Expr Patterns. 2003;3(6):777–83.
17. Weisbrod D, Khun SH, Bueno H, Peretz A, Attali B. Mechanisms underlying the cardiac pacemaker: the role of SK4 calcium-activated potassium channels. Acta Pharmacol Sin. 2016;37(1):82–97.
18. DiFrancesco D. Funny channels in the control of cardiac rhythm and mode of action of selective blockers. Pharmacol Res. 2006;53(5):399–406.
19. Hagiwara N, Irisawa H, Kasanuki H, Hosoda S. Background current in sino-atrial node cells of the rabbit heart. J Physiol. 1992;448:53–72.
20. Krapivinsky G, Gordon EA, Wickman K, Velimirovic B, Krapivinsky L, Clapham DE. The G-protein-gated atrial K+ channel IKACh is a heteromultimer of two inwardly rectifying K(+)-channel proteins. Nature. 1995;374(6518):135–41.
21. Wickman K, Krapivinsky G, Corey S, et al. Structure, G protein activation, and functional relevance of the cardiac G protein-gated K+ channel, IKACh. Ann N Y Acad Sci. 1999;868:386–98.
22. DiFrancesco D, Ducouret P, Robinson RB. Muscarinic modulation of cardiac rate at low acetylcholine concentrations. Science. 1989;243(4891):669–71.

23. Tamargo J, Caballero R, Gomez R, Valenzuela C, Delpon E. Pharmacology of cardiac potassium channels. Cardiovasc Res. 2004;62(1):9–33.
24. Stern MD, Capogrossi MC, Lakatta EG. Spontaneous calcium release from the sarcoplasmic reticulum in myocardial cells: mechanisms and consequences. Cell Calcium. 1988;9(5–6):247–56.
25. Bogdanov KY, Vinogradova TM, Lakatta EG. Sinoatrial nodal cell ryanodine receptor and na(+)-ca(2+) exchanger: Molecular partners in pacemaker regulation. Circ Res. 2001;88(12):1254–8.
26. van Campenhout MJ, Yaksh A, Kik C, et al. Bachmann's bundle: a key player in the development of atrial fibrillation? Circ Arrhythm Electrophysiol. 2013;6(5):1041–6.
27. Dobrzynski H, Anderson RH, Atkinson A, et al. Structure, function and clinical relevance of the cardiac conduction system, including the atrioventricular ring and outflow tract tissues. Pharmacol Ther. 2013;139(2):260–88.
28. Hancox J, Yuill K, Mitcheson J, Convery M. Progress and gaps in un- derstanding the electrophysiological properties of morphologically normal cells from the cardiac atrioventricular node. Int J Bifurcat Chaos. 2003;13:3675–91.
29. Greener ID, Tellez JO, Dobrzynski H, et al. Ion channel transcript expression at the rabbit atrioventricular conduction axis. Circ Arrhythm Electrophysiol. 2009;2(3):305–15.
30. Greener ID, Monfredi O, Inada S, et al. Molecular architecture of the human specialised atrioventricular conduction axis. J Mol Cell Cardiol. 2011;50(4):642–51.
31. Li J. Alterations in cell adhesion proteins and cardiomyopathy. World J Cardiol. 2014;6(5):304–13.
32. Meens MJ, Kwak BR, Duffy HS. Role of connexins and pannexins in cardiovascular physiology. Cell Mol Life Sci. 2015;72(15):2779–92.
33. Desplantez T, McCain ML, Beauchamp P, et al. Connexin43 ablation in foetal atrial myocytes decreases electrical coupling, partner connexins, and sodium current. Cardiovasc Res. 2012;94(1):58–65.
34. Sato PY, Musa H, Coombs W, et al. Loss of plakophilin-2 expression leads to decreased sodium current and slower conduction velocity in cultured cardiac myocytes. Circ Res. 2009;105(6):523–6.
35. Shu J, Zhou J, Patel C, Yan GX. Pharmacotherapy of cardiac arrhythmias—basic science for clinicians. Pacing Clin Electrophysiol. 2009;32(11):1454–65.
36. Hirano Y, Moscucci A, January CT. Direct measurement of L-type Ca2+ window current in heart cells. Circ Res. 1992;70(3):445–55.
37. January CT, Riddle JM. Early afterdepolarizations: mechanism of induction and block. A role for L-type Ca2+ current. Circ Res. 1989;64(5):977–90.
38. Nattel S, Maguy A, Le Bouter S, Yeh YH. Arrhythmogenic ion-channel remodeling in the heart: heart failure, myocardial infarction, and atrial fibrillation. Physiol Rev. 2007;87(2):425–56.
39. Bers DM. Cardiac sarcoplasmic reticulum calcium leak: basis and roles in cardiac dysfunction. Annu Rev Physiol. 2014;76:107–27.
40. Comtois P, Kneller J, Nattel S. Of circles and spirals: bridging the gap between the leading circle and spiral wave concepts of cardiac reentry. Europace. 2005;7(Suppl 2):10–20.
41. Allessie MA, Bonke FI, Schopman FJ. Circus movement in rabbit atrial muscle as a mechanism of tachycardia. III. the "leading circle" concept: a new model of circus movement in cardiac tissue without the involvement of an anatomical obstacle. Circ Res. 1977;41(1):9–18.
42. Rensma PL, Allessie MA, Lammers WJ, Bonke FI, Schalij MJ. Length of excitation wave and susceptibility to reentrant atrial arrhythmias in normal conscious dogs. Circ Res. 1988;62(2):395–410.
43. Li D, Fareh S, Leung TK, Nattel S. Promotion of atrial fibrillation by heart failure in dogs: atrial remodeling of a different sort. Circulation. 1999;100(1):87–95.
44. Aguilar M, Nattel S. The past, present, and potential future of sodium channel block as an atrial fibrillation suppressing strategy. J Cardiovasc Pharmacol. 2015;66(5):432–40.
45. Kneller J, Kalifa J, Zou R, et al. Mechanisms of atrial fibrillation termination by pure sodium channel blockade in an ionically-realistic mathematical model. Circ Res. 2005;96(5):e35–47.
46. Kalifa J, Jalife J, Zaitsev AV, et al. Intra-atrial pressure increases rate and organization of waves emanating from the superior pulmonary veins during atrial fibrillation. Circulation. 2003;108(6):668–71.
47. Cuculich PS, Wang Y, Lindsay BD, et al. Noninvasive characterization of epicardial activation in humans with diverse atrial fibrillation patterns. Circulation. 2010;122(14):1364–72.
48. Narayan SM, Krummen DE, Shivkumar K, Clopton P, Rappel WJ, Miller JM. Treatment of atrial fibrillation by the ablation of localized sources: CONFIRM (conventional ablation for atrial fibrillation with or without focal impulse and rotor modulation) trial. J Am Coll Cardiol. 2012;60(7):628–36.
49. Haissaguerre M, Hocini M, Denis A, et al. Driver domains in persistent atrial fibrillation. Circulation. 2014;130(7):530–8.